MICRO/MESO-ANALYSIS OF POLYMER COMPOSITES WITH DAMAGE EVOLUTION

Fernand Ellyin, Zihui Xia and Yunfa Zhang

Department of Mechanical Engineering, University of Alberta
Edmonton, Alberta, Canada T6G 2G8
fernand.ellyin@ualberta.ca

Abstract

The micro/meso-mechanical approach for composites is commonly based on the analysis of a representative volume element or a so-called repeated unit cell (RUC). Through analysis of the RUC model one can predict not only macroscopic mechanical properties but also microscopic damage initiation and its propagation in composites. In this paper, we present an overview of our contributions in the following three essential areas in the micro/meso-mechanical analyses: (1) a unified form of periodic boundary conditions for the RUC modelling; (2) a nonlinear viscoelastic constitutive model for polymer matrix materials; and (3) a post-damage constitutive model based on the concept of smeared crack. Application examples combining the above three topics are presented, in which three types of glass/epoxy laminates are analyzed using finite element method. The predicted results are compared with experimental data and they are in good agreement.

Introduction

Composite materials are widely used in advanced structures in aeronautics, astronautics, automotives, marine, petrochemical and many other industries due to their superior properties over conventional industrial materials. In the past couple of decades many researchers have devoted considerable effort to evaluate macro-mechanical properties of composites by using micro/meso-mechanical modelling methods. The latter method provides overall behaviour of the composites from known properties of the reinforcing phase (particles, fibre or fibre yarns) and the matrix phase (polymers, metals) through analysis of a representative volume element (RVE) or a repeated unit cell (RUC) model, see Aboudi (1991), Nemat-Nasser and Hori (1993). Furthermore, damage in composites generally occurs in a microscopic scale and its effect is manifested progressively into meso- and macro-scales. Micro/meso-mechanical modelling can also be used to study damage initiation and growth in composites.

There are three essential prerequisites for successful micro/meso-mechanical analyses of composites, viz: (1) An appropriate RUC model must be selected and correct periodical boundary conditions should be applied to the RUC model. (2) The constitutive models must accurately describe the mechanical behaviour of the constituents, especially of the matrix material. (3) Appropriate damage criteria for different damage mechanisms and post-damage constitutive model should be introduced to simulate damage initiation and propagation in composites.

For many composite materials, such as fibrous laminates and textile composites, the microstructure can be envisioned as a periodic array of RUC. Therefore in the micro/meso-analysis based on a RUC, the equilibrium equation should be solved under appropriate periodic boundary conditions. Valid periodic boundary conditions should ensure the compatibility of the neighbouring RUCs, i.e. both displacement and traction continuity conditions should be met. However, there still exist ambiguities in application of correct periodic boundary conditions. For example, in cases of shear loading or multiaxial loading in which shear stress is involved, homogeneous boundary conditions (plane-remains-plane or uniform boundary tractions) were applied to the RUC in some previous publications. Many researchers, e.g. Sun and Vaidya (1996), Yuan et al. (1997), Xia et al. (2003a), have pointed out

M. Pandey et al. (eds), Advances in Engineering Structures, Mechanics & Construction, 505–516.

that the homogeneous boundary conditions will over- or under-estimate the effective modulus, since by applying homogeneous boundary conditions, the displacement and traction continuity conditions can not always be satisfied at the same time.

Since the micro/meso-mechanical analyses are based on properties of individual constituents of the composite, an accurate constitutive model of each constituent becomes a prerequisite in attempting to predict the composite behaviour. Although the reinforcing phases, such as fibres, ceramic particles behave elastically for most of their stress-strain range, the polymer matrices are viscoelastic or viscoelastic-viscoplastic materials. The analysis of Hashin (1966) demonstrated that the viscoelastic effect in a unidirectional fibre composite is significant for axial shear, transverse shear and transverse uniaxial stress, for which the influence of matrix is dominant. Comprehensive experimental studies on an epoxy polymer (Hu et al. 2003, Shen et al. 2004) have indicated that these materials exhibit complex time- and loading-history-dependent properties. The viscoelastic effects become even more pronounced under conditions of high temperature, sustained loading and/or high stress level. Therefore, it is necessary to develop an accurate constitutive model for the polymer matrix material.

Due to co-existence of multi-phase materials with quite different mechanical properties, damage mechanisms of composites become more complicated. The initiation and evolution of the damages are essentially in the microscopic scale. Therefore, micro/meso-mechanical approaches are desirable to capture these damage mechanisms. The polymer matrices usually have much lower strength and stiffness than the reinforcing phases. Some damage modes (matrix micro-cracking, fiber/matrix interfacial debonding) could occur at relatively low applied loads or even during the manufacturing process. However, certain degree of damages may be tolerated in composites before the structural failure modes (delamination, fiber fracture) occur. Therefore, it is essential for damage analysis of composites to be able to identify different damage modes, to predict damage evolution within each mode and between different modes. To this end, appropriate damage criteria and post-damage constitutive relations are required.

In this paper, our recent contributions in the aforementioned three areas for polymeric composites will be elucidated. A unified form of periodic boundary conditions for any multiaxial loading conditions will be presented first, and uniqueness of the solution by applying the unified periodic boundary conditions on the RUCs will be proved. For an epoxy polymer matrix a nonlinear viscoelastic constitutive model in differential form has been developed based on comprehensive multiaxial experimental test data. The nonlinear viscoelasticity is described through introduction of a modulus function and a time-scale factor. A post-damage constitutive model based on the concept of smeared crack has also been introduced to simulate the behaviour after damage initiation. It permits crack description in terms of stress-strain relations and stiffness reduction in particular orientations instead of the common element-death method in FEM codes. Application examples combining the above three essential topics will be presented, in which three types of glass/epoxy laminates (45° unidirectional, cross-ply, and ±45° angle-ply) will be analyzed using finite element method. The predicted results are compared with experimental data and it is shown that they are in good agreement.

Unified Periodic Boundary Conditions

Consider a large sample of periodic inhomogeneous body (composite) as shown in Fig. 1. The body has two length scales, a global (macroscopic) length scale, *D*, which is of the order of the size of the body, and a local (microscopic) length scale, *d*, which is proportional to the wavelength of the variation of the microstructure. Correspondingly

$$\delta = d / D << 1 \tag{1}$$

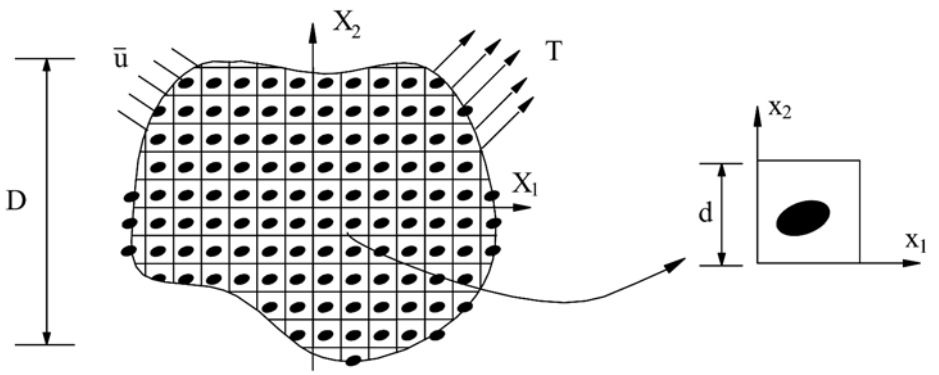

Fig. 1 RUC from a periodic composite.

Obviously, any function *f* in the body depends on two variables, *global (macroscopic) coordinates* X_i for the body and the *local (microscopic) coordinates* x_i for the unit cell. For small strain elasticity, the boundary value problem for the *composite body* can be defined as the following, from which the unknown field quantities, stress σ_{ij}, strain ε_{ij} and displacements u_i can be solved:

$$\sigma_{ij,j} = 0 \tag{2}$$

$$\sigma_{ij} = C_{ijkl}\varepsilon_{kl} \tag{3}$$

$$\varepsilon_{kl} = \frac{1}{2}(u_{k,l} + u_{l,k}) \tag{4}$$

$$\sigma_{ij}n_j = T_i \quad \text{on } \partial_\sigma, \qquad u_i = \bar{u}_i \quad \text{on } \partial_u \tag{5}$$

The boundary value problem has the feature that C_{ijkl} varies very rapidly within a short wavelength (order of *d*) on the global length scale X_i and therefore it is difficult to find a solution that solves the global problem and accounts for the local oscillation at the same time. For example, in a FEM solution, assuming roughly each unit cell should have several hundred elements to accurately capture the large variations due to the heterogeneity of the microstructure, then for the entire composite laminate or structure, the number of elements needed will increase by several orders. Hence, there is a motivation to seek a simplified solution. Since the composite body can be envisioned as a periodical array of the RUCs, it is adequate to obtain a solution based on an individual RUC. This implies that beyond a boundary layer of the composite body, each RUC in the composite has the same deformation mode and there is no separation or overlap between the neighbouring RUCs. That is, the stress and strain fields are periodic as the microstructure (Suquet, 1987).

Since the whole body, thus each unit cell is in balance, the equilibrium equation, Eqn. (2) and Eqns. (3)-(4) still apply in a RUC with volume *V*. However, the boundary conditions on the boundary of the RUC, ∂ , should be properly determined. In the case of periodic media, the microscopic fields have to fulfill suitable periodicity conditions ensuring continuity of boundary displacements and tractions across adjacent cells. According to Suquet (1987), the displacement field for a periodic structure can be expressed as:

$$u_i(x_1, x_2, x_3) = \bar{\varepsilon}_{ij}x_j + u_i^*(x_1, x_2, x_3) \tag{6}$$

In the above, $\bar{\varepsilon}_{ij}$ is the global strain tensor of the periodic structure and the first term on the right side represents a linear distributed displacement field. The second term on the right side is a periodic function from one RUC to another. In addition, for a periodic RUC, the tractions on the opposite boundary surfaces should also meet the continuity condition, i.e.

$$\sigma_{ij}(P)n_j(P) = -\sigma_{ij}(Q)n_j(Q) \tag{7}$$

where *P* and *Q* are two periodic points (with the same in-plane coordinates) on the two opposite boundary surfaces, **n** is the unit outward normal vector to the surfaces, see Fig. 1. Note that the global strain $\bar{\varepsilon}_{ij}$ in Eqn. (6) and the corresponding global stress $\bar{\sigma}_{ij}$ can be defined as the averages over the RUC volume *V*:

$$\bar{\sigma}_{ij} = \frac{1}{V}\int_V \sigma_{ij}(x_1, x_2, x_3)\,dV \tag{8}$$

$$\bar{\varepsilon}_{ij} = \frac{1}{V}\int_V \varepsilon_{ij}(x_1, x_2, x_3)\,dV \tag{9}$$

where $\sigma_{ij}(x_1, x_2, x_3)$ and $\varepsilon_{ij}(x_1, x_2, x_3)$ are local (microscopic) stress and strain defined in the RUC.

Equations (6) and (7) are the periodic boundary conditions for a RUC. Together with the Eqns. (2), (3) and (4), we complete the boundary value problem for the RUC. This boundary value problem is well-posed, as shown e.g. in Suquet (1987). However, the periodic part of displacement, $u_i^*(x_1, x_2, x_3)$, in Eqn. (6) is usually unknown prior to the solution, thus it is not convenient to apply Eqn. (6) directly as displacement boundary conditions. In Xia et al. (2003a), a unified form of periodic boundary conditions for any multiaxial loading and suitable for finite element analysis is developed. For the sake of brevity only the conclusions are cited here. Interested readers are encouraged to consult the reference for further details and illustrative examples.

For any RUC, its boundary surfaces must always appear in parallel pairs, the displacements of two periodic points on a pair of parallel opposite boundary surfaces can be written as

$$u_i(P) = \bar{\varepsilon}_{ij}x_j(P) + u_i^*(P) \tag{10}$$

$$u_i(Q) = \bar{\varepsilon}_{ij}x_j(Q) + u_i^*(Q) \tag{11}$$

In the above "*P*" and "*Q*" identify the two corresponding points on a pair of two opposite parallel boundary surfaces of the RUC, see Fig. 1.

Note that $u_i^*(x_1, x_2, x_3)$ is a periodic function, i.e. its value is the same for two corresponding points at the two parallel boundaries (periodicity), therefore, the difference between the above two equations is

$$u_i(P) - u_i(Q) = \bar{\varepsilon}_{ij}[x_j(P) - x_j(Q)] = \bar{\varepsilon}_{ij}\Delta x_j \tag{12}$$

Since $\Delta x_j = x_j(P) - x_j(Q)$ are constants for each pair of the parallel boundary surfaces, hence, for a specified $\bar{\varepsilon}_{ij}$, the right side becomes constants. Equation (12) is a special type of displacement boundary conditions. Instead of giving known values of boundary displacements, it specifies the

displacement-differences between two periodic points at opposite boundaries. Obviously, the application of Eqn. (12) will guarantee the continuity of displacement field, i.e. the neighboring RUCs cannot separate or encroach into each other at the boundaries after the deformation.

Furthermore, it has been proved in Xia et al. (2006) that if a RUC is analyzed by using a displacement-based finite element method, the application of only Eqn. (12) can guarantee the uniqueness of the solution and thus Eqn. (7) are automatically satisfied. For the sake of brevity only the conclusions are cited here.

Theorem: In a displacement-based FEM analysis, by applying the unified displacement-difference periodic boundary conditions on a RUC, a unique solution is obtained.

Lemma 1 For a fixed periodic structure, different RUC's may be defined, however, by applying the unified displacement-difference periodic boundary conditions, Eqn. (12), in the displacement-based FEM analysis, the solution will be independent of the choice of the RUCs.

Lemma 2 The solution obtained by applying the unified displacement-difference periodic boundary conditions, Eqn. (12), in the displacement-based FEM analysis, will also meet the traction continuity conditions, Eqn. (7).

It is noted that the unified periodic boundary conditions, Eqn. (12), can be easily applied in a FEM as the nodal displacement constraint equations. It is also noted that the proposed unified periodic boundary conditions are in the form of global strains. In the case of given global stresses, or a combination of the global stresses and strains, a proper proportion between the global strains must be applied. The required proportion can be determined without any difficulty through an iterative procedure, see the examples to follow.

One can also note that the derivation and proof procedures for the proposed unified periodic boundary conditions are not dependent on the properties of the constituent materials of the composites. Therefore, they can be applied to nonlinear micro/meso-mechanical analyses of the composites under any combination of multiaxial loads.

Nonlinear Viscoelastic Constitutive Model for Epoxy Polymers

Based on comprehensive experimental data (Hu et al. 2003, Shen et al. 2004) a new nonlinear viscoelastic model has been recently developed by the authors (Xia et al. 2003b, Xia et al. 2005). Here only a brief description will be given.

For the uniaxial stress state, the model can be represented by a finite number of nonlinear 'Kelvin-Voigt type' elements and a linear spring element, connected in series (Fig. 2). The constitutive equations, generalized to the multiaxial stress state, are sumarized below:

$$\{\dot{\varepsilon}_t\} = \{\dot{\varepsilon}_e\} + \{\dot{\varepsilon}_c\} \tag{13}$$

$$\{\dot{\varepsilon}_c\} = \sum_{i=1}^{n} \left(\frac{[A]}{E_i \tau_i} \{\sigma\} - \frac{1}{\tau_i} \{\varepsilon_{ci}\} \right) \tag{14}$$

$$\{\dot{\sigma}\} = E[A]^{-1} \{\dot{\varepsilon}_e\} \tag{15}$$

In the above, $\{\dot{\varepsilon}_t\}$, $\{\dot{\varepsilon}_e\}$, $\{\dot{\varepsilon}_c\}$, $\{\dot{\sigma}\}$ are the total strain-rate, elastic strain-rate, creep strain-rate, and stress-rate vectors (each contains six components, respectively). E is an elastic modulus which is assumed to be constant and $[A]$ is a matrix related to the value of Poisson's ratio, defined by

$$[A]=\begin{bmatrix} 1 & -\upsilon & -\upsilon & 0 & 0 & 0 \\ -\upsilon & 1 & -\upsilon & 0 & 0 & 0 \\ -\upsilon & -\upsilon & 1 & 0 & 0 & 0 \\ 0 & 0 & 0 & 1+\upsilon & 0 & 0 \\ 0 & 0 & 0 & 0 & 1+\upsilon & 0 \\ 0 & 0 & 0 & 0 & 0 & 1+\upsilon \end{bmatrix} \tag{16}$$

In Eqn. (14) $\tau_i = \eta_i / E_i$ $(i = 1, 2, \cdots, n)$ denotes the retardation time, E_i is the spring stiffness and η_i is the dashpot viscosity for the *i*-th 'Kelvin-Voigt type' element, respectively. Based on Eqn. (14), the retardation time τ_i has a damped exponential character as in an exponential-type function. Its value determines the time duration after which contribution from the individual 'Kelvin-Voigt type' element becomes negligible. Therefore, the number of the 'Kelvin-Voigt type' elements adopted in the constitutive equation depends on the required time range. For simplicity, we introduce a time scale factor α, and assume that

$$\tau_i = (\alpha)^{i-1}\tau_1 \tag{17}$$

In this way all τ_i are related through the scale factor α. A time span of order of *n* would be covered, if *n* 'Kelvin-Voigt type' elements were chosen and the value of α is taken to be 10.

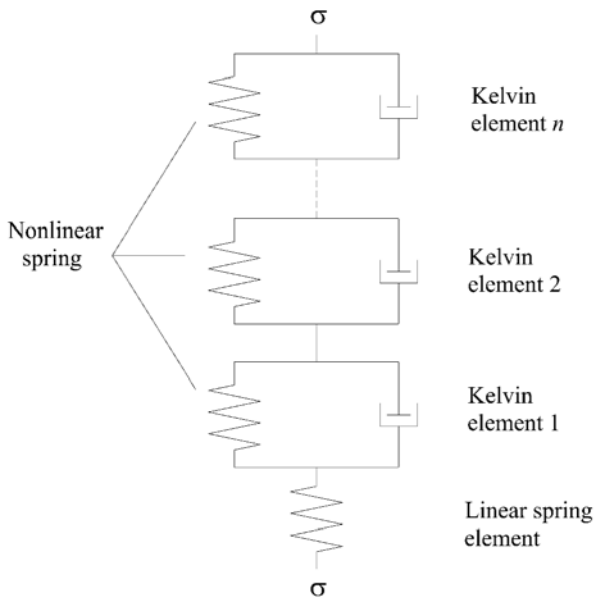

Fig. 2 A uniaxial visoelastic model represented by a finite series of 'Kelvin-Voigt type' elements coupled with an elastic spring.

The description of the nonlinear behaviour in the current model is achieved by letting E_i's be functions of the current equivalent stress, σ_{eq}. Furthermore, a single function form for all E_i's is assumed, i.e.

$$E_i = E_1(\sigma_{eq}) \tag{18}$$

with

$$\sigma_{eq} = \frac{(R-1)I_1 + \sqrt{(R-1)^2 I_1^2 + 12RJ_2}}{2R} \tag{19}$$

where $I_1 = \sigma_1 + \sigma_2 + \sigma_3$ is the first invariant of the stress tensor, $J_2 = s_{ij}s_{ij}/2$ is the second invariant of the deviatoric stress and R is the ratio of compressive to tensile 'yield stress'. Note that when $R = 1$, then Eqn. (19) reduces to the von Mises equivalent stress, $\sigma_{eq} = \sqrt{3J_2}$.

The five constants ($E, \upsilon, \alpha, \tau_1$, R) and the functional form of $E_1(\sigma_{eq})$ can be determined from uniaxial creep curves tested at different stress levels by a simple procedure described in Xia et al. (2003b).

A distinct feature of this constitutive model is its capacity to distinguish between loading and unloading cases by introducing a stress memory surface and a corresponding switch rule. The stress memory surface is defined as:

$$f_m^{\sigma}(\sigma_{ij}) - R_{mem}^2 = \frac{3}{2}s_{ij}s_{ij} - R_{mem}^2 = 0 \tag{20}$$

where $s_{ij} = \sigma_{ij} - \frac{1}{3}\sigma_{kk}\delta_{ij}$ are the deviatoric stress components. The radius of the memory surface, R_{mem}, is determined by the maximum von Mises stress level experienced by the material during its previous loading history, i.e. $R_{mem} = \sqrt{(3s_{ij}s_{ij}/2)_{\max}}$. Therefore, for a monotonic loading from a stress free state, the memory surface will expand isotropically with the increasing stress level. If σ_{ij}^t is the current stress point, $d\sigma_{ij}^t$ is the stress increment at time t, and $(\frac{\partial f}{\partial \sigma_{ij}})_{s_{ij}=s_{ij}^t}$ represents the direction of the normal to the memory surface at the current stress point, then the criterion to distinguish the loading/unloading cases is defined as follows:

- if the current stress point is on the memory surface and $(\frac{\partial f}{\partial \sigma_{ij}})_{\sigma_{ij}^t} \cdot d\sigma_{ij}^t \geq 0$, this signifies a loading case;
- if the current stress point is on the memory surface and $(\frac{\partial f}{\partial \sigma_{ij}})_{\sigma_{ij}^t} \cdot d\sigma_{ij}^t < 0$, then a switch from loading to unloading occurs;
- if the current stress point is inside the memory surface, i.e. $f_m^{\sigma}(\sigma_{ij}^t) - R_{mem}^2 < 0$, it is then an unloading case.

For the loading case the spring stiffness of the 'Kelvin-Voigt type' elements is defined as a function of the equivalent stress, $E_i = E_1(\sigma_{eq})$. For the unloading case, it is assumed that E_i remains the same during the entire unloading process, and its value is that of the E_i at which the switch from loading to unloading took place.

Post-Damage Constitutive Model Based on the Concept of Smeared Crack

Upon increasing the applied load, micro-cracks will develop in the matrix. These cracks cause reduction in stiffness of the laminate. In contrast to a predefined single dominant crack in isotropic materials, the orientation and location or even numbers of cracks in a laminate is unknown, thus this makes it difficult to deal with such cracks through the classical fracture mechanics approach. Instead, the so-called 'smeared crack' approach will be used. In this approach the reduction of load bearing capacity induced by a crack is described by stress-strain softening relationship. In this manner the discontinuity caused by a crack is smeared out, and this procedure can be implemented into a FEM code.

Once a crack is formed, it is assumed that it cannot transfer normal and shear stresses across the crack surfaces, i.e. σ_1, σ_{12} and $\sigma_{13} \to 0$. The subscript 1 denotes the Cartesian axis perpendicular to the crack plane while 2 and 3 are in the crack plane. However, the ability to transfer the other stress components is not affected by the crack formation. Let the stress and strain vectors in the local (crack) coordinate system be designated by $\{\sigma\}^{cr}$ and $\{\varepsilon\}^{cr}$, respectively. Thus, the post-damage constitutive model in the crack coordinate system is

$$\{\Delta\sigma\}^{cr} = E_t[D]\{\Delta\varepsilon\}^{cr} - \chi[B]\{\sigma\}^{cr} \tag{21}$$

or written in its full form:

$$\begin{pmatrix} \Delta\sigma_1 \\ \Delta\sigma_2 \\ \Delta\sigma_3 \\ \Delta\sigma_{12} \\ \Delta\sigma_{23} \\ \Delta\sigma_{31} \end{pmatrix}^{cr} = E_t \begin{pmatrix} \beta Z_1 & 0 & 0 & 0 & 0 & 0 \\ 0 & Z_1 & Z_2 & 0 & 0 & 0 \\ 0 & Z_2 & Z_1 & 0 & 0 & 0 \\ 0 & 0 & 0 & \beta Z_3 & 0 & 0 \\ 0 & 0 & 0 & 0 & Z_3 & 0 \\ 0 & 0 & 0 & 0 & 0 & \beta Z_3 \end{pmatrix} \begin{pmatrix} \Delta\varepsilon_1 \\ \Delta\varepsilon_2 \\ \Delta\varepsilon_3 \\ \Delta\gamma_{12} \\ \Delta\gamma_{23} \\ \Delta\gamma_{31} \end{pmatrix}^{cr} - \chi \begin{pmatrix} 1 & 0 & 0 & 0 & 0 & 0 \\ 0 & 0 & 0 & 0 & 0 & 0 \\ 0 & 0 & 0 & 0 & 0 & 0 \\ 0 & 0 & 0 & 1 & 0 & 0 \\ 0 & 0 & 0 & 0 & 0 & 0 \\ 0 & 0 & 0 & 0 & 0 & 1 \end{pmatrix} \begin{pmatrix} \sigma_1 \\ \sigma_2 \\ \sigma_3 \\ \sigma_{12} \\ \sigma_{23} \\ \sigma_{31} \end{pmatrix}^{cr} \tag{22}$$

In the above,

$$Z_1 = \frac{1-\upsilon}{(1+\upsilon)(1-2\upsilon)},\ Z_2 = \frac{\upsilon}{(1+\upsilon)(1-2\upsilon)},\ Z_3 = \frac{1}{2(1+\upsilon)}, \tag{23}$$

E_t is the modulus of the epoxy under uniaxial tensile loading at the instant of damage initiation, β is a small number which represents the loss of the stiffness in these three particular stress directions and the constant χ allows the three stress components to decrease to a near zero value in a sufficiently short time duration.

Application Examples

The response of three types of glass fiber/epoxy polymer matrix laminates subject to a tensile loading are presented herein, see Ellyin and Kujawski (1995), Zhang et al. (2005). These are: (1) a unidirectional laminate under 45° off-axis loading; (2) a [0°/90°]ns cross-ply laminate under transverse loading, and (3) a [±45°]ns angle-ply laminate under tensile loading, see Fig. 3(a), (b), (c), respectively. The 45° off-axis tension on the unidirectional laminate (Fig. 3a) and the tensile load on

the $[\pm 45°]_{ns}$ angle-ply laminate (Fig 3c) result in combined normal and shear traction boundary conditions as shown in figures with

$$\bar{\sigma}_x = \bar{\sigma}_y = \bar{\tau}_{xy} = 0.5\bar{\sigma} \tag{24}$$

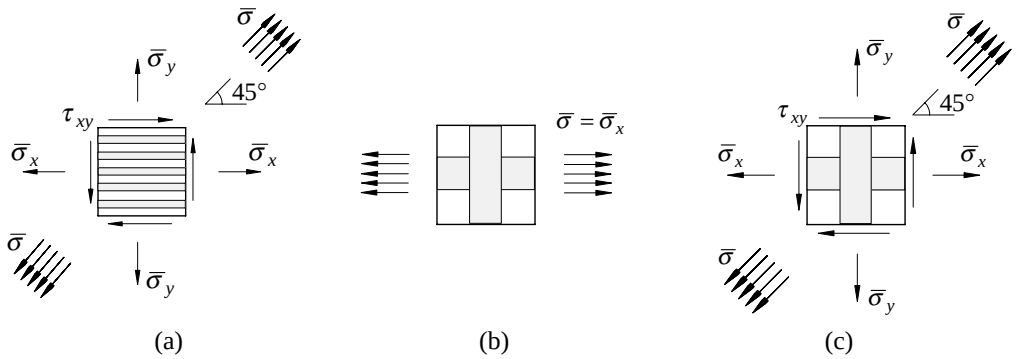

(a) (b) (c)

Fig. 3 (a) a unidirectional laminate under 45° off-axis loading; (b) a cross-ply laminate under transverse loading; (c) a [±45°]ns angle-ply laminate under tensile loading.

The RUC for the unidirectional laminate is a unit cube containing a cylindrical fiber and the RUCs for both $[0°/90°]_{ns}$ cross-ply laminate and $[\pm 45°]_{ns}$ angle-ply laminate are the same consisting of two cubes with the two cylindrical fibers at an angle of 90° (Fig. 4a, b).

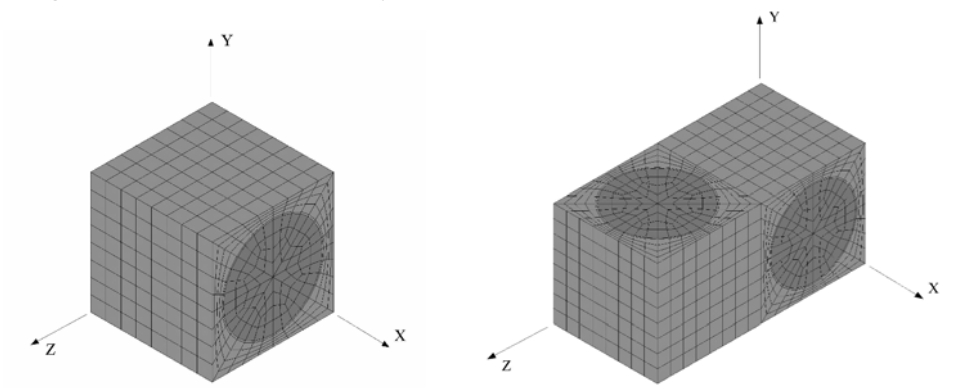

(a) (b)

Fig. 4 Meshed RUCs for (a) unidirectional laminate and for (b) cross-ply laminate and [±45°]ns angle-ply laminate.

The finite element code ADINA was used to conduct the numerical analysis. The nonlinear viscoelastic constitutive model of the epoxy matrix and the post-damage constitutive model were implemented into the code through its user-defined subroutine. It is to be noted that in Eqn. (24) the multiaxial loads are the global stress components applied to the RUCs. The applied periodic boundary conditions, Eqn. (12), are in the form of global strain components. An iterative procedure is required to ensure proper proportion of the increments of the global strain components are applied so that Eqn. (24) is satisfied at each time step. The iteration procedure is as follows.

(i) For each time step, Δt , we apply a set of trial global strain increments, $\Delta\bar{\varepsilon}_{ij}$.

(ii) The solution gives the stress distribution in the RUC, so the global stress components are the average values over the volume V of the RUC (see Eqn. 8.)
(iii) Equation (24) is checked and, if it is satisfied (within a certain error limit), then one proceeds to the next time step. If not, new values of $\Delta\bar{\varepsilon}_{ij}$ are obtained and the steps (i) to (iii) are repeated. For a small time step, it could be assumed that the increments of $\Delta\bar{\varepsilon}_{ij}$ are proportional to the corresponding increment of average stress components, then the new values of $\Delta\bar{\varepsilon}_{ij}$ can be estimated.

Two damage mechanisms were considered in the analyses, i.e. matrix cracking and fibre breaking. For the epoxy polymer matrix, a maximum principal strain criterion was adopted, i.e. if $\varepsilon_1 \geq \varepsilon_{cr} = 4.8\%$, the matrix element was assumed to be damaged and subsequently the post-damage constitutive relation would be used. (The manufacturer did not provide the failure strain for the neat resin, the value assumed here was taken from another resin system). For the glass fiber, the average axial strain of the fibre was monitored and if it exceeded a prescribed maximum value, i.e. $\bar{\varepsilon}_{fa} \geq \varepsilon_{f\max} = 2.3\%$ then the fiber was assumed to have fractured and the calculation was then terminated. The above critical strain values were taken from experimental data and the fiber volume fraction of the laminates was assumed to be 52.5%.

Prediction of Stress-Strain Curves for the Three Types of Laminates

Figures 5 and 6 display the predicted global stress-strain curves of the three types of laminates and the comparison with the test results. All the calculations use the same set of material constants and the same set of constants used in the post-damage constitutive model. The test specimens were made of "Scotchply 1003" prepregs of 3M Company. The test data of cross-ply laminates were taken from the technical data of the 3M Company and that of the [±45°]ns angle-ply laminates and unidirectional laminates (UDC) under 45° off-axis loading were from Ellyin and Kujawski (1995). It is seen that the predictions of the drastically different responses of the three types of laminates are in good agreement with the experimental data.

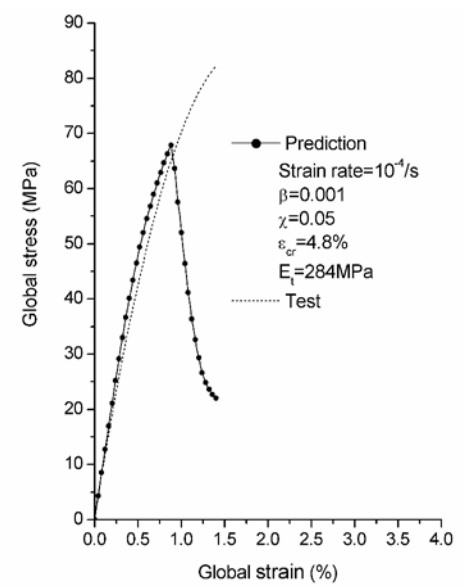

Fig. 5 Predicted stress-strain curve of a UDC under 45° off-axis tensile loading.

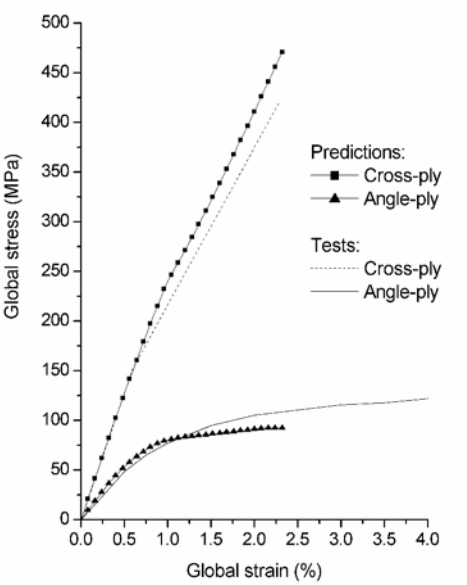

Fig. 6 Predicted stress-strain curves of cross-ply and angle-ply laminates.

In the case of the unidirectional laminate, it is noted that the predicted trend is in good agreement with the test results, Fig. 5. The predicted initial stiffness is 10.1 GPa, and the maximum load is 68 MPa, while the corresponding test results are 10.1 GPa and 82 MPa.

The effect of viscoelastic behavior of the matrix is manifested by the nonlinearity of the stress-strain curve, which is noticeable once the stress exceeds 40 MPa (about 0.5% strain). Since damage has not yet occurred at this load level (for the unidirectional laminate, damage initiates at the peak of the stress-strain curve), therefore this nonlinearity is mainly caused by the viscoelasticity of the epoxy matrix.

For the cross-ply and angle-ply laminates the test and predicted results are shown in Figure 6. For the cross-ply laminate, a bilinear stress-strain curve is predicted in which the two 'moduli' are approximately 25.5 GPa and 17.4 GPa. The corresponding test values are 25.5 GPa and 15.6 GPa, respectively. The knee between the two straight lines corresponds to the load level at which the transverse cracking of matrix occurs in the laminate. And the final failure of the specimen is due to the fracture of fibers in the 0° plies. From the technical data of the 'Scotchply', the test value of tensile strength of cross-ply laminate is 480 MPa, and the present prediction of 470 MPa is very close to that of the test. Note, however, that for the other two laminates, no fiber fracture occurs within the strain range of the present calculations.

The unique nonlinear stress-strain curve of the [±45°]ns laminate is also well predicted. For example, the predicted initial stiffness of 10.1 GPa agreed very well with the test value of 10.1 GPa. In contrast to the unidirectional laminate under 45° off-axis loading which failed at a relatively low global strain of 0.9%, at the same strain level, the [±45°]ns laminate is capable of carrying the applied load albeit at a reduced stiffness. However, prior to the 'yield' point, the stress-strain curve also manifested a nonlinear response. Since the damage has not yet occurred at this load level (50 MPa), this nonlinearity is mainly caused by the viscoelasticity of the epoxy matrix. Note that the nonlinearity of the stress-strain curve has different causes at different strain levels: at lower strain levels, it is mainly caused by the viscoelasticity of the matrix, while at higher strain values, the onset of damage and its evolution is the main contributor to the nonlinear response. Finally, it should be noted that the simulation is carried out up to about 2.3% applied global strain. Thereafter, it is difficult to continue the simulation, since the local deformation is very large and the present FEM model is based on the small deformation formulation.

Conclusions

To perform an effective micro/meso-mechanical analysis of composite materials and to obtain reliable predictions, the following three prerequisites are essential:

(1) Correct periodic boundary conditions must be applied to the repeated unit cells (RUCs).
- A unified form of periodic boundary conditions for RUCs of composites has been presented.
- Application of the proposed periodic boundary conditions can guarantee both the displacement and traction continuity. The solution is also independent on the choice of RUCs.

(2) The constitutive models must accurately represent the constituents' behaviours.
- A nonlinear viscoelastic constitutive model has been developed for epoxy polymers.
- The model is capable of predicting complicated time- and loading-history-dependent response of the polymer matrix materials.

(3) Proper damage criteria and post-damage constitutive model must be included in the analyses to simulate different damage modes in composite materials.
- A post-damage constitutive model based on smeared crack concept has been developed.

- Initiation and propagation of matrix cracking in composites are well simulated by using this post-damage constitutive model.

Acknowledgements

The Work presented here is supported, in part, by grants to F.E and Z.X. from the Natural Sciences and Engineering Research Council (NSERC) of Canada.

References

Aboudi, J., (1991). *Mechanics of Composite Materials, A Unified Micromechanical Approach*. Elsevier Science Publishers, Amsterdam.

Ellyin, F., Kujawski, D. (1995). Tensile and fatigue behaviour of glass fibre/epoxy laminates. *Construction and Building Materials*, **9**, 425-430.

Hashin, Z. (1966). Viscoelastic fiber reinforced materials. *AIAA Journal*, **4**, 1141-1147.

Hu, Y., Xia, Z, Ellyin, F. (2003). Deformation behavior of an epoxy resin subjected to multiaxial loadings, part I: experimental investigations. *Polymer Engineering & Science*, **43**, 721-733.

Nemat-Nasser S., Hori M. (1993). *Micromechanics: Overall Properties of Heterogeneous Materials*. Elsevier Science Publishers, Amsterdam.

Shen, X., Xia, Z., Ellyin, F. (2004). Cyclic deformation behavior of an epoxy polymer, part I: experimental investigation. *Polymer Engineering & Science*, **44**, 2240-2246.

Sun, C. T., Vaidya, R. S. (1996). Prediction of composite properties from a representative volume element. *Composites Science and Technology*, **56**, 171-179.

Suquet, P. (1987). Elements of homogenization theory for inelastic solid mechanics. In: Sanchez-Palencia, E., Zaoui, A., (eds.). *Homogenization Techniques for Composite Media*. Springer-Verlag, Berlin, 194-275.

Xia, Z., Zhang, Y., Ellyin, F. (2003a). A unified periodical boundary condition for representative volume elements of composites and applications. *International Journal of Solids and Structures*, **40**, 1907-1921.

Xia, Z, Hu, Y., Ellyin, F. (2003b). Deformation behavior of an epoxy resin subjected to multiaxial loadings, part II: constitutive modeling and predictions. *Polymer Engineering & Science*, **43**, 734-748.

Xia, Z., Shen, X., Ellyin, F. (2005). Cyclic deformation behavior of an epoxy polymer, part II: prediction of constitutive model. *Polymer Engineering & Science*, **45**, 103-113.

Xia, Z., Zhou, C., Yong. Q., Wang, X. (2006). On selection of repeated unit cell model and application of unified periodic boundary conditions in micro-mechanical analysis of Composites. *International Journal of Solids and Structures*, **43**, 266-278.

Yuan, F. G., Pagano, N. J., Cai, X. (1997). Elastic moduli of brittle matrix composites with interfacial debonding. *International Journal of Solids and Structures*, **34**, 177-201.

Zhang, Y., Xia, Z., Ellyin, F. (2005). Viscoelastic and damage analyses of fiber reinforced polymer laminates by micro/meso-mechanical modeling. *Journal of Composite Materials*, **39**, 2001-2022.

3M Minnesota Mining & Manufacturing CO., Technical Data of 'Scotchply' Reinforced Plastic Type 1002 & 1003, St. Paul, Minnesota, USA.